

Generation of Singlet Oxygen from Fragmentation of Monoactivated 1,1-Dihydroperoxides

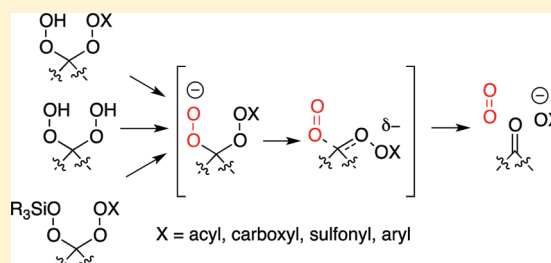
Jiliang Hang,[†] Prasanta Ghorai,^{†,§} Solaire A. Finkenstaedt-Quinn,[‡] Ilhan Findik,[‡] Emily Sliz,[‡] Keith T. Kuwata,[‡] and Patrick H. Dussault^{*,†}

[†]Department of Chemistry, University of Nebraska–Lincoln, Lincoln, Nebraska 68588-0304, United States

[‡]Department of Chemistry, Macalester College, Saint Paul, Minnesota 55105-1899, United States

Supporting Information

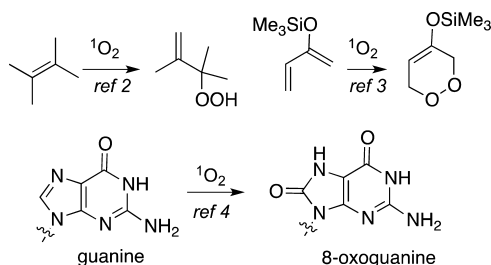
ABSTRACT: The first singlet excited state of molecular oxygen ($^1\text{O}_2$) is an important oxidant in chemistry, biology, and medicine. $^1\text{O}_2$ is most often generated through photosensitized excitation of ground-state oxygen. $^1\text{O}_2$ can also be generated chemically through the decomposition of hydrogen peroxide and other peroxides. However, most of these “dark oxygenations” require water-rich media associated with short $^1\text{O}_2$ lifetimes, and there is a need for oxygenations able to be conducted in organic solvents. We now report that monoactivated derivatives of 1,1-dihydroperoxides undergo a previously unobserved fragmentation to generate high yields of singlet molecular oxygen ($^1\text{O}_2$). The fragmentations, which can be conducted in a variety of organic solvents, require a geminal relationship between a peroxyanion and a peroxide activated toward heterolytic cleavage. The reaction is general for a range of skeletal frameworks and activating groups and, via in situ activation, can be applied directly to 1,1-dihydroperoxides. Our investigation suggests the fragmentation involves rate-limiting formation of a peroxyanion that decomposes via a Grob-like process.



INTRODUCTION

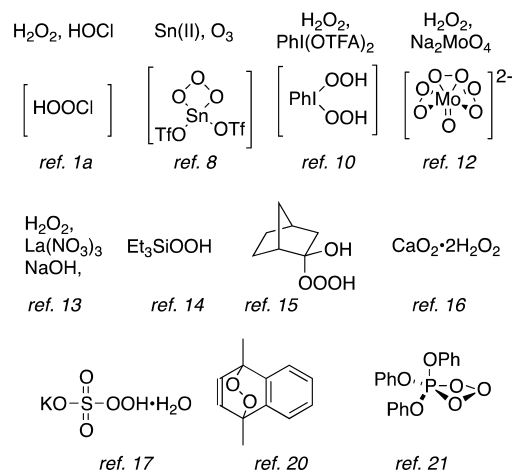
Singlet molecular oxygen ($^1\text{O}_2$) is an important oxidant in chemistry, biology, and medicine and the source of energy for chemical oxygen–iodine (COIL) lasers.^{1a–c} Several typical reactions are illustrated in Scheme 1.^{2–4}

Scheme 1. Examples of $^1\text{O}_2$ Reactivity



$^1\text{O}_2$ is most commonly generated through dye-sensitized excitation of ground-state dioxygen ($^3\text{O}_2$).^{1b,5} However, preparative application can be limited by the need for high-volume photo-reactors, as well as by safety issues associated with reactions under oxygen.⁶ Following the discovery of the chemical generation of $^1\text{O}_2$ from the reaction of hydrogen peroxide and bleach,⁷ a number of methods for “dark oxygenation” have been reported based upon decomposition of ozone,⁸ hydrogen peroxide,^{1a,9–13} hydrotrioxides,^{14,15} and several inorganic peroxides.^{16,17} The majority of these methods require the use of water-enriched media, conditions associated with a very short $^1\text{O}_2$ lifetime.¹⁸

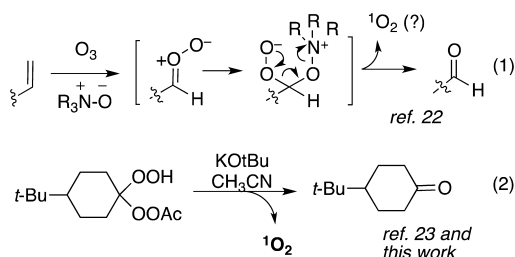
However, preparative oxidations have been achieved for relatively reactive substrates using biphasic or emulsion conditions.¹⁹ Generation of $^1\text{O}_2$ in organic solvents has been achieved through thermal decomposition of calcium peroxide (suspension),¹⁶ arene endoperoxides,²⁰ phosphite ozonides,²¹ silyl hydrotrioxides,¹⁴ and alkyl hydrotrioxides.¹⁵ However, the latter class of reagents are often thermally unstable and must be prepared immediately prior to reaction. Major classes of reagents for chemical generation of $^1\text{O}_2$ are overviewed below.



Received: November 23, 2011

Published: January 11, 2012

Our interest in this area arose during investigations of a “reductive ozonolysis” of alkenes.²² This transformation was hypothesized to involve nucleophilic addition of amine *N*-oxides to short-lived carbonyl oxides to generate peroxyanion/oxyammonium acetals. These previously unknown intermediates were surmised to undergo fragmentation to generate the observed “reduction” products, along with a molecule of ¹O₂, and a molecule of amine (eq 1). Reasoning that a similar

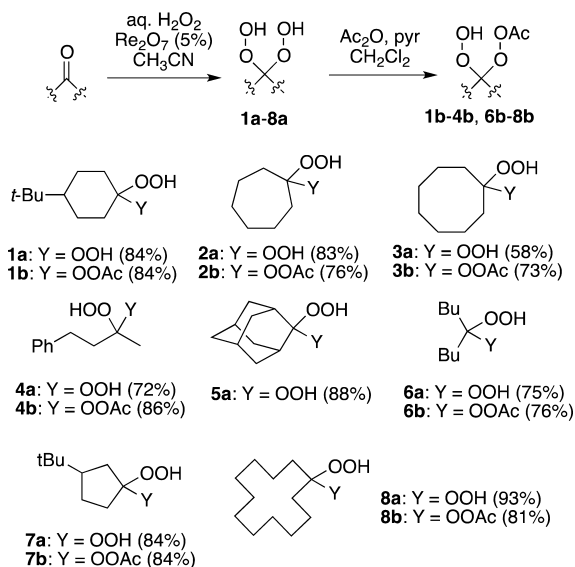


fragmentation should be possible for any species featuring a geminal relationship between a peroxyanion and a heterolytically activated O–X bond, we explored the reactivity of monoesters of readily available 1,1-dihydroperoxides. Deprotonation of these species resulted in rapid fragmentation accompanied by highly efficient liberation of ¹O₂ (eq 2).²³ We now describe our investigations into the scope and mechanism of this process.

RESULTS

Range of Acetal/Ketal Scaffolds. 1,1-Bishydroperoxides **1a–8a** were prepared through Re(VII)-promoted acetalization of the corresponding ketones (Scheme 2).²⁴ Monoacetylation

Scheme 2. Synthesis of 1,1-Dihydroperoxides and Derived Monoesters



with acetic anhydride and pyridine furnished isolable monoesters (**1b–8b**);²⁵ the exception was adamantane dihydroperoxide (**5a**), which instead underwent ring expansion to a lactone. 1,1-Dihydroperoxides derived from aldehydes (not shown) reacted to form highly polar byproducts, presumably reflecting E₁cb fragmentation of peresters bearing an adjacent C–H.²⁶

Thermal Stability. Dihydroperoxide **1a**, which melts without decomposition at 78–80 °C and is not detonated by a sharp hammer blow, undergoes a highly exothermic decomposition when heated beyond 100 °C. Monoacetate **1b** is stable for prolonged periods at freezer temperature and for days at room temperature but undergoes an exothermic decomposition beginning at approximately 76 °C (Figure 1). Monocarbonate **1d** undergoes partial

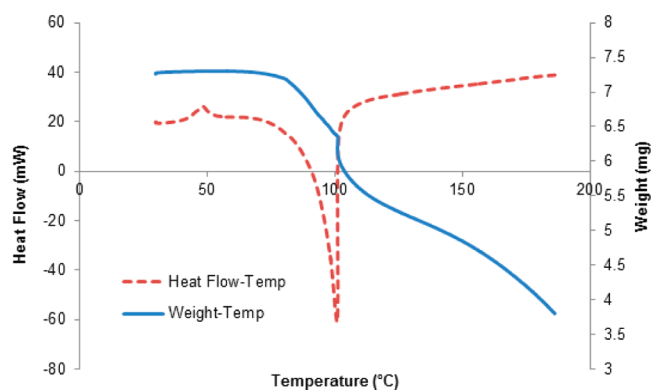
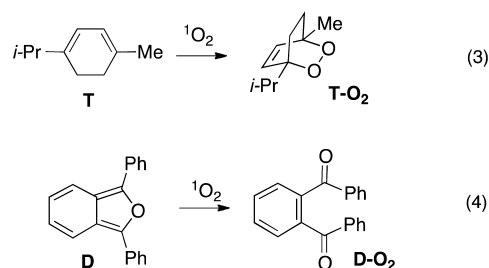


Figure 1. Thermal stability of dihydroperoxide monoester **1b**.

decomposition within days at room temperature to form a substituted caprolactone and undergoes exothermic decomposition when heated above 70 °C.

Assay for ¹O₂. The release of ¹O₂ was quantified by chemical reaction with terpinene (**T**) or diphenylisobenzofuran (DPBF, **D**). Terpinene (**T**) undergoes addition of ¹O₂ to form the stable endoperoxide ascaridole (**T-O₂**, eq 3).²⁷ Furan **D** undergoes an



even faster addition to generate diketone **D-O₂** via an unstable endoperoxide (eq 4). **T-O₂** and **D-O₂** are easily quantified through isolation or by NMR or GC/MS analysis in the presence of an internal standard. Details are provided in Supporting Information.

Variation of the Bisperoxyacetal Skeleton. We next investigated the generality of the fragmentation across a range of peroxyacetal skeletons. Solutions of monoesters **1b–4b** and **6b–8b** were decomposed with TBAF in the presence of 0.5 equiv of terpinene (Table 1); the relative stoichiometry was chosen to facilitate product separation. Addition of base was accompanied by the disappearance (TLC) of the monoesters and the appearance of the corresponding ketone and **T-O₂**. The yield of trapped ¹O₂ varied little with peroxyacetal structure. By comparison, a 1,1-dihydroperoxide (**1a**) did not react under the reaction conditions.

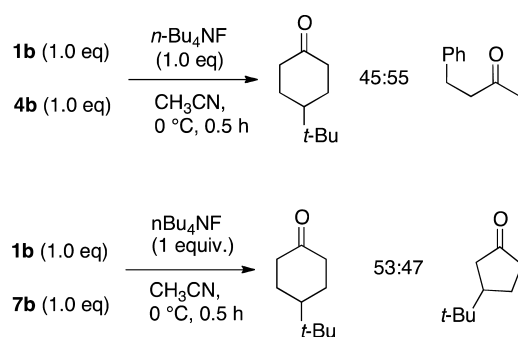
Influence of Peroxyacetal Backbone on Relative Reactivity. The decomposition of mixtures of dihydroperoxide monoesters in the presence of a limiting amount of TBAF revealed little difference in reactivity between acyclic and cyclic substrates or between cyclic substrates possessing different amounts of ring strain (Scheme 3).

Table 1. Influence of Peroxyacetal Backbone

$$\begin{array}{c} \text{R} \\ \diagup \\ \text{C} \\ \diagdown \\ \text{R} \end{array} \begin{array}{l} \text{OOH} \\ \text{OOAc} \end{array} + \text{T (0.5 eq)} \xrightarrow[\text{CH}_3\text{CN (r.t.), 0.08h}]{n\text{-Bu}_4\text{NF (1.2 eq)}} \text{T-O}_2$$

monoperester or bisOOH	yield of T-O ₂ ^a (%)
1b	26
2b	26
3b	23
4b	31
5b	27
7b	24
8b	23
1a	NR

^aRelative to monoperester

Scheme 3. Influence of Scaffold on Reactivity^a^aProducts analyzed by GC/MS.

Influence of Solvent. Decomposition of monoester **1b** in a number of solvent systems (Table 2) revealed the yield of

Table 2. Influence of Solvent on Trapped ¹O₂

$$\text{1b (1.0 equiv)} + \text{T (0.5 equiv)} \xrightarrow[\text{solvent, r.t., 0.08h}]{\text{base (1.2eq)}} \text{T-O}_2$$

solvent	base	yield of T-O ₂ ^a (%)
CH ₃ CN	<i>n</i> -Bu ₄ NF	26
CHCl ₃	<i>n</i> -Bu ₄ NF	17
CDCl ₃	<i>n</i> -Bu ₄ NF	35
acetone-d ₆	<i>n</i> -Bu ₄ NF	33
C ₆ D ₆	<i>n</i> -Bu ₄ NF	30
C ₆ F ₆	<i>n</i> -Bu ₄ NF	7 ^b
C ₆ F ₆	KOtBu	1 ^b
C ₆ F ₆ / CH ₃ CN (9:1)	<i>n</i> -Bu ₄ NF	24
C ₆ F ₆ / CH ₃ CN (1:1)	<i>n</i> -Bu ₄ NF	36
C ₆ F ₁₄ / CH ₃ CN (1:1) ^c	<i>n</i> -Bu ₄ NF	28
Freon-113/CH ₃ CN (1:1)	<i>n</i> -Bu ₄ NF	39

^aBased upon **1b**. ^bLimited reagent solubility. ^cBiphasic.

dioxygen transfer (as T-O₂) to be increased in solvents associated with greater ¹O₂ lifetime.¹⁸ The exception was for perfluorinated media, in which the reaction appeared limited by reagent solubility. However, improved yields were possible in fluorocarbon/CH₃CN mixtures.

Order of Addition. In early experiments involving decomposition of monoperester **1b**,²³ we had observed the yield of ¹O₂ to vary with the relative order of addition of KOtBu and perester, suggesting the possibility of disproportionation to form poorly

reactive bisperesters (vidua infra). However, a reinvestigation of the phenomenon using peracetate **1b** and TBAF revealed insignificant differences (Table 3).

Table 3. Influence of Order of Addition of Reagents

$$\begin{array}{l} \text{1b (1.0 equiv)} \\ + \\ \text{T (0.5 equiv)} \end{array} \xrightarrow[\text{CH}_3\text{CN, 0 }^\circ\text{C, 0.16h}]{n\text{-Bu}_4\text{NF (1.2 eq, in THF)}} \text{T-O}_2$$

conditions	yield of T-O ₂ ^a (%)
add <i>n</i> -Bu ₄ NF to solution of 1b and T	35
add 1b to solution of <i>n</i> -Bu ₄ NF and T	38

^aBased upon **1b**.

Range of Activating Groups. Base-promoted decomposition of a perbenzoate (**1c**) and a percarbonate (**1d**) proceeded rapidly to furnish yields of trapped ¹O₂ similar to those observed for the peracetate (Table 4). Attempts to

Table 4. Investigation of Other Peracyl Activating Groups

$$\text{di-OOH 1a} \xrightarrow{\text{reagent}} \begin{array}{c} \text{HO} \\ | \\ \text{O} \\ | \\ \text{C} \\ | \\ \text{O} \\ | \\ \text{C} \\ | \\ \text{O} \\ | \\ \text{X} \end{array} \xrightarrow[\text{T, CH}_3\text{CN}]{\text{TBAF}} \text{T-O}_2$$

1c: X = Ph
1d: X = OEt

reagent	yield of 1c or 1d (%)	yield of T-O ₂ ^a (%)
PhCOCl	1c (37)	24
EtOC(O)Cl	1d (76)	20
PhNCO	dec	
TsCl	dec	

^aBased upon T-O₂ vs stoichiometry of **1c** or **1d**

prepare the analogous percarbonate or persulfonate led only to ring-expansion.

Influence of Base/Counterion. As shown in Table 5, the decomposition of **1b** in the presence of LiN(TMS)₂ resulted in

Table 5. Influence of Base

$$\text{t-Bu-Cyclohexane ring with OOH and OOAc} + \text{T (0.5 eq)} \xrightarrow[\text{CH}_3\text{CN, 0 }^\circ\text{C, 0.16h}]{\text{base (1.2 eq)}} \text{T-O}_2$$

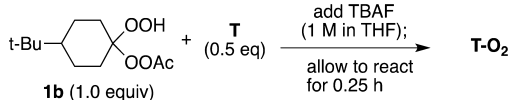
base	yield of T-O ₂ ^a (%)
KOtBu	30
LiN(SiMe ₃) ₂ (in THF)	4.1
<i>n</i> Bu ₄ NF (in THF)	35

^aBased upon **1b**.

much lower yields of ¹O₂ trapping compared to reactions involving the comparably basic KOtBu or TBAF.

Effect of Temperature and Rate of Addition. The base-promoted decomposition of the 1,1-dihydroperoxide monoesters is rapid; for example, rapid (1–2 s) injection of a 1 M THF solution of TBAF into a rapidly stirring solution of monoester **1b** (1 M in THF) results in immediate effervescence. Although the decomposition of monoester **1b** proceeds significantly faster at higher temperatures, the yield of trapped ¹O₂ is improved at lower temperatures (Table 6, entries 1–4). Slowing the rate of

Table 6. Influence of Temperature and Rate of Addition



entry	T (°C)	solvent	addition mode	yield of T-O ₂ ^a (%)
1	rt	THF	<i>b</i>	10
2	0	THF	<i>b</i>	13
3	-40	THF	<i>b</i>	19
4	-78	THF	<i>b</i>	24
5	rt	CH ₃ CN	<i>b</i>	24
6	rt	CH ₃ CN	<i>c</i>	42

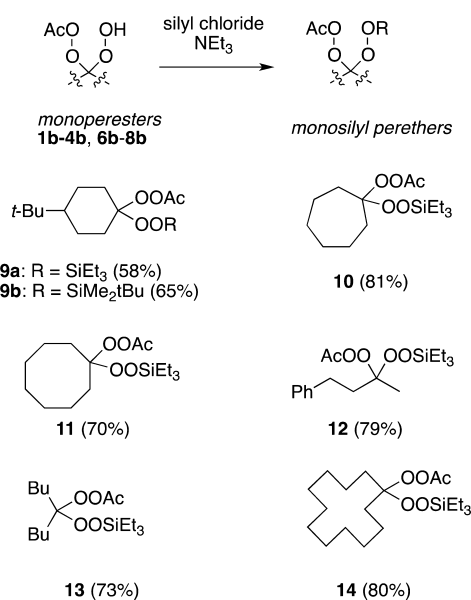
^aRelative to perester. ^bSyringe ($\leq 10^{-3}$ h). ^cSyringe pump (0.25 h).

reagent addition resulted in a significant increase in the yield of trapped ¹O₂ (entries 5 and 6).

Attempted Gas-Phase Transfer. The inverted relationship between the yield of oxygen transfer and the rate of peroxide decomposition (Table 6, entries 5 and 6) led us to investigate whether ¹O₂ could be escaping into the gas phase. The head-space of a septum-covered flask containing an acetonitrile solution of perester **1b** was exhausted via a short Teflon tube into an acetonitrile solution of terpinene (T). Rapid (≤ 10 s) addition of TBAF/THF into the solution of monoester led to vigorous effervescence and net efflux of a high volume of gas through the receiving solution. However, no significant amount of ascaridole (T-O₂) was detected.

Generation of the Peroxanion via Nucleophilic Desilylation. We investigated an alternative route to the presumed peroxanion intermediate through nucleophilic desilylation. Monotrialkylsilylated substrates were readily available via silylation of the monoesters (Scheme 4). Curiously, the perester

Scheme 4. Synthesis of Silylated Peresters



carbonyl remained invisible by ¹³C NMR despite use of pulse delays (≥ 5 s) or the addition of Ni(acac)₂ as a relaxation agent.²⁸ The perester carbonyl could be observed as a single sharp signal at 167.8 ppm if spectra were acquired at ≤ 40 °C (**9a**, **9b**, **11**). We are unsure as to the basis of this phenomenon, which was

not encountered with either the monoesters (e.g., **1b**) or a bisperester (**16**, *vide infra*).

Reaction of the silylated monoesters with TBAF in the presence of a trapping agent resulted in yields of transferred ¹O₂ equal to or exceeding those observed through deprotonation of the dihydroperoxide monoesters (Table 7).

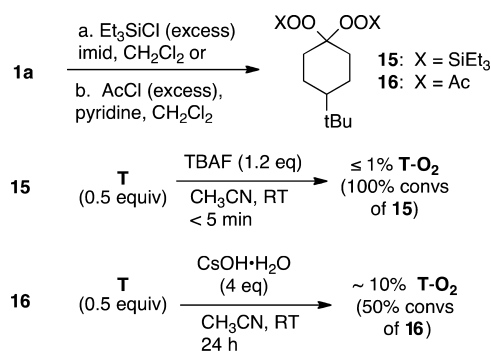
Table 7. Fragmentation of Silylated Dihydroperoxide Monoesters

subs	SiR ₃	T or D (0.5 equiv)	TBAF/THF (1.2 eq) CH ₃ CN, rt	trap	T-O ₂ or D-O ₂ yield ^a (%)
9a	SiEt ₃			D	33
9b	TBS			D	29
9b	TBS			T	25
9b	TBS			D	25
10	SiEt ₃			D	34
11	SiEt ₃			D	37
12	SiEt ₃			D	41
13	SiEt ₃			D	38
14	SiEt ₃			D	28

^aBased on silylated perester.

Reactivity of Bissilyl and Bisacyl Derivatives. Preparations of bissilyl and bisacyl derivatives of dihydroperoxide **1a** are illustrated in Scheme 5. The bistriethylsilyl derivative (**15**)

Scheme 5. Reactivity of Bissilyl and Bisacyl Derivatives of 1,1-Dihydroperoxides



was an oily compound that decomposed at ~ 140 °C. The bisacyl derivative (**16**) was a solid that melted without decomposition at 54–56 °C.²⁹ Saponification of **16** with cesium hydroxide in CH₃CN resulted in reformation of the parent ketone and generation of ¹O₂. Bissilyl ether **15** was decomposed by *n*-Bu₄NF without apparent transfer of oxygen.

Tandem Activation and Fragmentation. Intrigued by the possibility of generating and decomposing the monoactivated bisperoxide intermediate in situ, we investigated the reactivity of dihydroperoxide **1a** toward four classes of activating agents: an electron-poor nitrile, a heteroaromatic known to undergo S_NAr reaction with tertiary hydroperoxides,³⁰ a sulfonyl chloride, and an acid anhydride. Our initial assay qualitatively monitored the formation of ketone upon addition of base to solutions containing the dihydroperoxide and the individual additive (Table 8). In each case, the addition of stoichiometric electrophile and excess KOTBu resulted in rapid conversion of **1a** to 4-*tert*-butylcyclohexanone without any evidence of intermediates. Although these reactions should in theory require only two equivalents of base, we found that four

Table 8. Investigation of Electrophiles for Activation/Fragmentation

activator	KOTBu (equiv)	time (h)	conversion ^a
CCl ₃ CN	2.0	0.75	incomplete
CCl ₃ CN	4.0	≤0.1	complete
triazene	2.0	>12	incomplete
triazene	4.0	≤0.1	complete
<i>p</i> -TsCl	2.0	0.3	incomplete
<i>p</i> -TsCl	4.0	≤0.1	complete
Ac ₂ O	2.0	0.5	incomplete
Ac ₂ O	4.0	0.25	complete

^aTLC and/or NMR

equivalents were invariably required to achieve complete consumption of the dihydroperoxide.

We next reinvestigated the most promising conditions in the presence of a trapping agent. The yields of oxygen transfer, which were as good as those obtained from the dihydroperoxide monoesters, were similar regardless of activating agent (Table 9).

Table 9. Oxygen Transfer via in Situ Activation

activator	time (min)	yield of D-O ₂ ^a (%)
CCl ₃ CN	5	36
triazene	5	39.5
<i>p</i> -TsCl	5	39
Ac ₂ O	5	31

^aRelative to dihydroperoxide 1a.

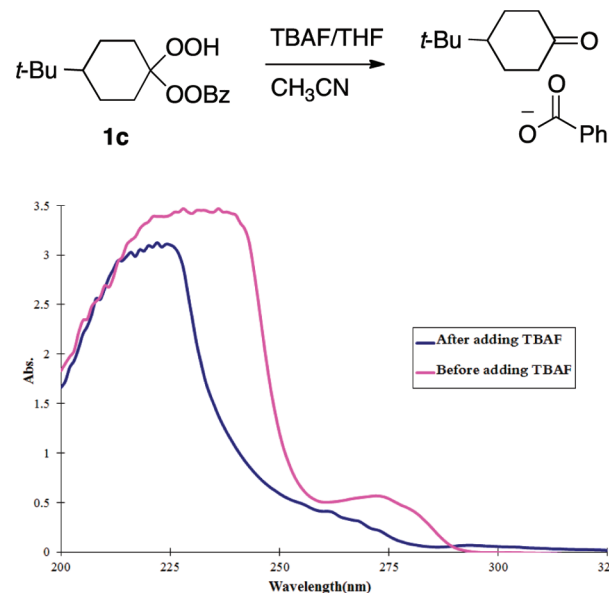
Preparative Reactions. Our experiments until this point had focused on the yield of liberated oxygen. We next investigated the amount of reagent necessary to completely consume a trapping reagent using either the fragmentation of a preformed perester (**1b**, **8b**) or the tandem activation/fragmentation of dihydroperoxide **1a**. As illustrated in Table 10, complete consumption of terpinene was generally possible with as little as 5 equiv of reagent.

Table 10. Investigation of Preparative Oxygenations

subs (equiv)	trap	reagents (equiv)	time (min)	product, yield ^a (%)
1b (5)	T	TBAF (5)	10	T-O ₂ (83)
1b (6)	T	TBAF (6)	10	T-O ₂ (100)
1b (2.5)	D	TBAF (2.5)	5	D-O ₂ (100)
1a (5)	T	triazene (5), KOTBu (20)	15	T-O ₂ (69)
1a (7)	T	triazene (7), KOTBu (28)	15	T-O ₂ (100)
8b (6)	T	TBAF (6)	10	T-O ₂ (100)

^aYield of T-O₂ or D-O₂.

Reaction Order and Apparent Rate Constant. The base-promoted decomposition of monoester **1c** was monitored at 272 nm (Figure 2). In the first experiment,

**Figure 2.** Monitoring rate of decompositions.

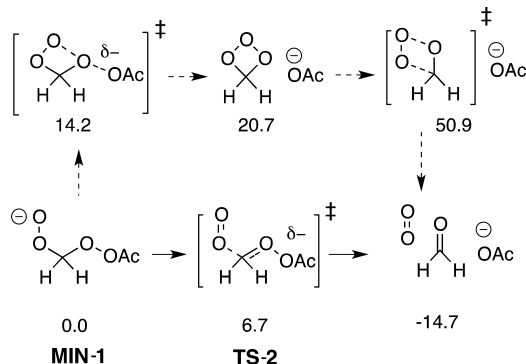
rapidly stirred THF solutions (0.5 mM) of dihydroperoxide monoester **1c** were mixed with THF solutions of TBAF ranging in concentration from 0.50 to 2.00 mM. The reaction solutions were then placed in the UV spectrophotometer, and the absorbance at 272 nm monitored for 1.0 min. Plotting the $\log[\text{TBAF}]_{\text{initial}}$ against the $-\log(\Delta_{\text{abs}})$ revealed an apparent reaction order of 0.94 in TBAF and a calculated rate constant of 10^2 L/mol-s; details are provided in the Supporting Information. Repeating the experiment with a constant concentration of TBAF and varying concentrations of **1c** indicated an order of 1.2 in peroxide and a calculated rate constant of 10^2 L/mol-s. Overall, the results support a mechanism that is first-order in both peroxide and base.

Theoretical Investigations of the Putative Fragmentation Step. The base-promoted fragmentation of the monoactivated 1,1-dihydroperoxides could conceivably involve either a concerted Grob-like fragmentation of a zwitterion or the formation and decomposition of an intermediate trioxetane.^{31a,b} The latter pathway cannot be simply disregarded. Dioxetanes are readily formed by intramolecular nucleophilic displacements of 2-hydroperoxide,³² while dioxiranes are generated with good efficiency from intramolecular attack of a hemiacetal oxygen on

an electrophilically activated peroxide.³³ We therefore turned to density functional theory (specifically, the B3LYP hybrid functional and the 6-31+G(d,p) basis set) to investigate each transition state (TS) and intermediate (MIN) involved in the decomposition of the monoactivated dihydroperoxides. We focused our efforts on heterolytic processes as fragmentations involving radical intermediates would be expected to generate $^3\text{O}_2$ and not $^1\text{O}_2$.

Decomposition of the Monoester. Comparison of the predicted zero-point corrected relative energies for transition states and intermediates in the decomposition of a peroxyanion found a concerted fragmentation to offer the lowest energy pathway for generation of $^1\text{O}_2$ and a carbonyl (Scheme 6). The alternative pathway is disfavored by the strain

Scheme 6. Available Pathways and Predicted Relative Energies (kcal/mol) for Fragmentation of a Deprotonated Monoester^a



^aEnergetics are based on the most stable conformer of each structure.

in the trioxetane intermediate, presumably reflecting electron pair repulsions, and by the high barrier for loss of $^1\text{O}_2$. (The combined energy of the trioxetane and acetate is 6.5 kcal/mol higher than the trioxetane formation transition state. This reflects the existence of an exit channel complex of the trioxetane and acetate that is bound by 16.3 kcal/mol.) For simplicity, calculations were performed on an unsubstituted acetal framework. Repeating the computations on a more substituted acetal framework (not shown) lowered the energies of most intermediates and transition states on the order of 5 kcal/mol but did not, in general, alter the relative energies of the transition states. The exception was the transition state for trioxetane formation, which increased significantly in energy for the more substituted scaffold. Optimized coordinates for calculated structures are provided in the Supporting Information.

Conformational Analysis of the Peroxyanion. Figure 3 shows the optimized geometries of two of the 12 possible conformers of the peroxyanion in the unsubstituted acetate system. There is a striking difference in energy between conformers MIN-1a (and the structurally and energetically similar MIN-1b, not shown) versus the remaining 10 conformers, exemplified by MIN-1c, all of which lie at least 8 kcal/mol higher in energy.³⁴

The most stable conformer (MIN-1a, Figure 3a) possesses two pairs of synclinal O–O and C–O bonds, allowing for hyperconjugation of oxygen lone pairs from O₂ and O₃ into neighboring C–O antibonding orbitals (C₁–O₃; C₁–O₂). The antiperiplanar orientation of the C₂–O₅ and O₃–O₄ bonds minimizes the repulsion between the lone pairs on O₃ and O₅.

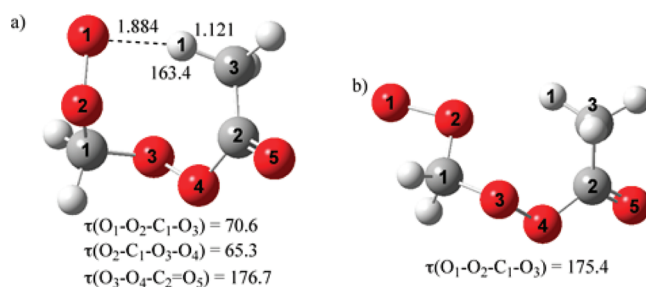


Figure 3. (a) Optimized geometry of the ground-state conformer, MIN-1a. (b) Optimized geometry of conformer MIN-1c. Bond lengths are in angstroms, and bond angles and dihedral angles are in degrees.

Several lines of evidence suggest the presence of a stabilizing intramolecular hydrogen bond between the anionic oxygen (O₁) and the C₃–H₁ bond. The O₁...H₁ distance is less than 1.9 Å, and the C₃–H₁ bond is 0.03 Å longer than the other two methyl C–H bonds. The C₃–H₁ bond also vibrates at a much lower frequency (2693 cm⁻¹) compared with the other hydrogen atoms on C₃ (~3100 cm⁻¹). These data support a normal hydrogen bond in which electron density from the peroxyanion is delocalized into the sigma antibonding orbital of the C–H bond. There is precedence for normal C–H hydrogen bonds in the literature.³⁵ Conformer MIN-1b (not shown) is structurally very similar to MIN-1a. In particular, MIN-1b also possesses an intramolecular hydrogen bond, with an O₁...H₁ distance of 1.851 Å. In contrast, the O₁–O₂ and C₁–O₃ bonds in conformer MIN-1c are antiperiplanar instead of synclinal (Figure 3b). This difference deprives MIN-1c of the intramolecular hydrogen bond and removes one of the hyperconjugative interactions, raising the energy of MIN-1c by 7–8 kcal/mol.³⁴

Conformational Analysis of the Grob-Like Transition States. The lowest energy conformer of the transition state for Grob fragmentation, TS-2 (Figure 4a), is predicted to lie only 6.7 kcal/mol higher in energy than the ground-state reactant conformer; TS-2 benefits from antiperiplanar O₂–C₁ and O₃–O₄ bonds. As described by Grob,^{31a,b} this arrangement facilitates fragmentation since electron density in the O₂–C₁ bond can be donated into the sigma antibonding orbital of the O₃–O₄ bond. Intrinsic reaction coordinate calculations reveal that TS-2 does not correlate directly with any of the reactant conformers (see the Supporting Information), but rather the unnumbered van der Waals complex shown in Figure 4b. This complex lies only 0.4 kcal/mol below the transition state in energy, and the excess –1 charge in the complex is evenly distributed between the OCH₂O and OC(O)CH₃ moieties.

Another fragmentation transition state, TS-2* (Figure 4c), which is only 0.7 kcal higher in energy than TS-2, is derived from the most stable peroxyanion conformer, MIN-1a (Figure 3a). TS-2* lacks antiperiplanar O₂–C₁ and O₃–O₄ bonds but is stabilized by a weak intramolecular hydrogen bond between O₁ and H₁: the C₃–H₁ bond is 0.01 Å longer than the other two methyl C–H bonds, and the C₃–H₁ stretch is ~200 cm⁻¹ to the red of the other methyl C–H stretches.

For a more substituted system (methine rather than methylene acetal), the two lowest energy transition states are structurally analogous to those shown in Figure 4. However, the methylated transition state lacking antiperiplanar O₂–C₁ and O₃–O₄ bonds, but possessing an intramolecular hydrogen bond,

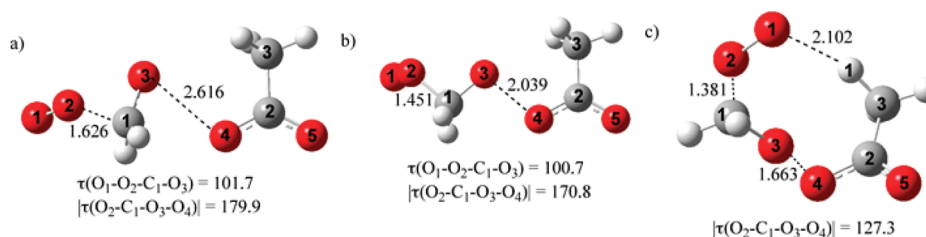
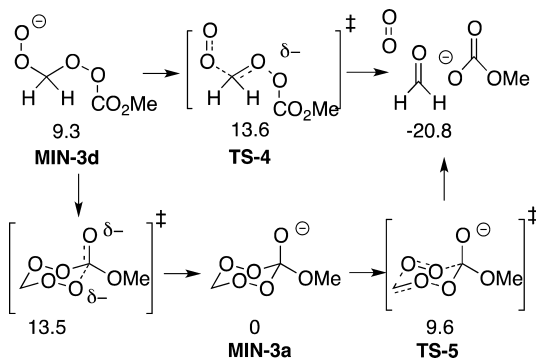


Figure 4. (a) Optimized geometry of the most stable conformer of TS-2. (b) Optimized geometry of the reactant complex leading to the most stable conformer of TS-2. (c) Optimized geometry of the second most stable transition-state conformer, TS-2*.

is slightly (0.8 kcal/mol) lower in energy than the one possessing antiperiplanar O₂–C₁ and O₃–O₄ bonds.

Pathways for Fragmentation of the Monopercarbonate. We were interested in whether the pathways for fragmentation varied with the nature of the electrophilic activating group. Scheme 7 shows calculated zero-point corrected

Scheme 7. Calculated Relative Energies (kcal/mol) for Selected Intermediates (MIN) and Transition States (TS) in Fragmentation of Percarbonates



relative energies for selected intermediates and transition states in the decomposition of a peroxyanion derived from a dihydroperoxide monopercarbonate, as modeled for the unsubstituted (formaldehyde acetal) backbone.³⁴ The methyl carbonate nucleofuge in the percarbonate stabilizes negative charge more effectively than the acetate leaving group in the perester, as indicated by a calculated ΔE of decomposition ~ 6 kcal/mol more exothermic than in the acetate series (compare Schemes 6 and 7). The two lowest energy pathways for liberation of ¹O₂ from the deprotonated monocarbonate are illustrated in Scheme 7. A third pathway involving an intermediate trioxetane, analogous to one illustrated in Scheme 6 for the monoester, was predicted to involve a very high energy transition state and is not described here.

Concerted fragmentation of the most stable conformer of the acyclic peroxyanion of the dihydroperoxide monocarbonate is calculated to occur with a significantly lower activation barrier (4.3 vs 6.7 kcal/mol) compared with the corresponding transformation of the perester (Scheme 6). We note that bond breaking in TS-4 (see Figure 5) is significantly less advanced than in the most stable transition state for the acetate system (TS-2, Figure 4a) and is comparable to the bond breaking that exists in the second most stable acetate conformer (TS-2*, Figure 4c). As is the case for the most stable peracetate transition state conformer, TS-4 (Figure 5) benefits from antiperiplanar O₂–C₁ and O₃–O₄ bonds. However, overlap of the σ (O₂–C₁) and σ^* (O₃–O₄) orbitals is not optimal, since

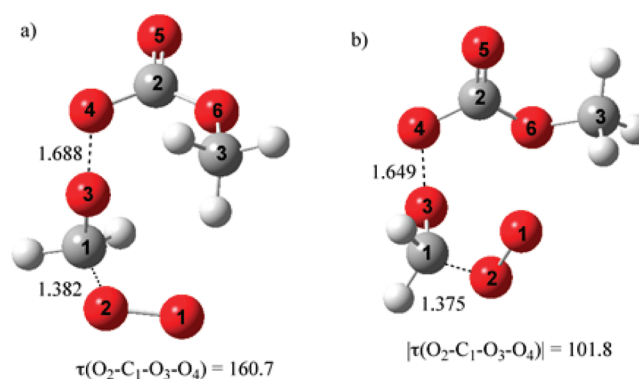


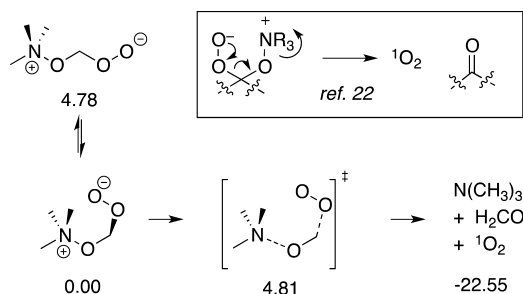
Figure 5. Optimized geometries of the most stable conformers of (a) TS-4 and (b) TS-5. Bond lengths are in angstroms, and bond angles and dihedral angles are in degrees.

the dihedral angle between the O₂–C₁ and O₃–O₄ bonds is significantly less than 180°.

The peroxyanion derived from the dihydroperoxide monopercarbonate can also undergo decomposition via a six-membered ring intermediate (Scheme 7). The barrier for cyclization to the 1,2,4,5-tetroxan-3-oxide is predicted to be nearly identical to that for fragmentation of the acyclic peroxyanion. The preference for the cyclic isomer is substantial: the ground state conformer of the tetroxane oxide (MIN-3a) is over 9 kcal/mol lower in energy than the most stable acyclic conformation (MIN-3d),³⁴ reflecting the significant number of hyperconjugative interactions between C–O sigma antibonding orbitals and oxygen lone pairs in the chairlike conformation of the cyclic isomer. Figure 5b shows the transition state, TS-5, for the fragmentation of the cyclic peroxide to generate a carbonyl, ¹O₂, and a methyl carbonate anion. The activation barrier for fragmenting the cyclic structure, while greater than that for fragmenting the acyclic peroxyanion (9.6 vs 4.3 kcal/mol), is still lower than that for ring-opening to the acyclic form. As was the case in the monoester series, fragmentation of a more substituted acetal is predicted to be more favorable by ~ 5 kcal/mol; however, there is predicted to be a minimal impact, typically less than 1 kcal/mol, on the relative energies of individual pathways.

Comparison with Intermediates in “Reductive” Ozonolysis. We also modeled analogous intermediates and transition states postulated to be involved in the fragmentation of zwitterionic peroxy/ammonium acetals during reductive ozonolyses (Scheme 8).²² As a result of a stabilizing electrostatic interaction, the zwitterionic acetal is predicted to strongly favor a ground-state conformation with a gauche O–C–O–O. The low-energy transition state for fragmentation lies less than 5 kcal/mol above the ground state; the fragmentation itself is predicted to be significantly downhill. (These calculations are based upon a zwitterionic acetal incorporating a fully substituted nitrogen; repeating these calculations on a species

Scheme 8. Calculated Energies for Decompositions of Zwitterionic Peroxyacetals

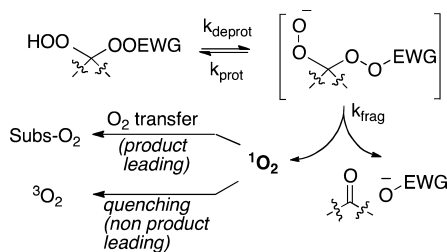


containing one or more N–H bonds predicted proton transfer would take place in preference to fragmentation).

DISCUSSION

The reactions described here constitute a new class of fragmentations involving a peroxyanion geminally linked to an electrophilically activated peroxide (Scheme 9).³⁶ The peroxyanion

Scheme 9. Mechanistic Overview



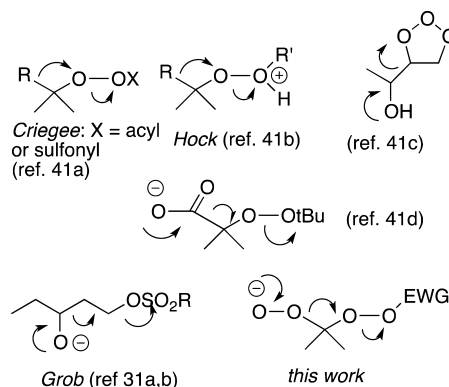
can be generated via deprotonation, desilylation, or deacylation. The higher yields observed in the presence of tetraalkylammonium or potassium counterions vs lithium point to the potential importance of anion dissociation, but must be interpreted with caution given the potential for different levels of $^1\text{O}_2$ quenching by the different bases and their protonated byproducts. The data from competition reactions suggests that deprotonation may be rate limiting.

The ability to achieve tandem activation and fragmentation of readily available 1,1-dihydroperoxides is noteworthy. Hydroperoxyimides, while not isolable, have been postulated as short-lived intermediates in epoxidations.³⁷ Alkylperoxytriazines, which have been prepared from tertiary hydroperoxides via $\text{S}_{\text{N}}\text{Ar}$ reactions, have mainly been of interest as radical initiators.³⁰

Relationship between Reaction Conditions and Efficiency of $^1\text{O}_2$ Transfer. The observation of more efficient oxygen transfer in deuterated or halogenated solvents is in keeping with the enhanced lifetime of $^1\text{O}_2$ in solvents lacking C–H, O–H, or N–H bonds.¹⁸ The failure of the results to scale linearly to $^1\text{O}_2$ lifetime results from the presence of the trapping substrate, by definition a potent quenching agent. The observation of improved trapping yields at reduced reaction temperatures is not unexpected. While the lifetime of $^1\text{O}_2$ in organic solvents varies little with temperature,³⁸ reaction of $^1\text{O}_2$ with electron-rich alkenes has a near-zero enthalpy of activation and a strongly negative entropy of activation;³⁹ photosensitized oxygenations are often quite rapid even at low temperatures.⁵ However, the observation of increased yields from a slower rate of fragmentation is not easily explained. Although rapid injection of reactants was associated with significant

effervescence, we could detect no evidence for transfer of $^1\text{O}_2$ into the gas phase. We therefore suspect that yields of oxygen transfer under conditions associated with higher $^1\text{O}_2$ flux are limited by self-quenching.⁴⁰

Relationship to Known Fragmentations. A number of heterolytic fragmentations involve formation of a new C–O bond through migration of a C–C σ bond with cleavage of an activated O–O bond.^{41a,b,c,d} These include the Criegee rearrangement of peresters,^{41a} the Hock rearrangement of protonated or Lewis acid-complexed peroxides,^{41b} the fragmentation of primary ozonides derived from allylic alcohols,^{41c} and the fragmentation of 2-hydroperoxycarboxylates.^{41d} Overall, the new fragmentation bears a close topological resemblance to the Grob fragmentation, an extended elimination reaction in which formation of C=O and C=C pi systems drives the cleavage of C–C and C–X σ bonds.^{31a,b} The fragmentations described above are likely to require a similar antiperiplanar alignment of the breaking peroxyanion C–O with the activated O–O bond.



CONCLUSIONS

The decomposition of monoactivated derivatives of 1,1-dihydroperoxides is established as a new peroxide fragmentation that provides an efficient means for preparative generation of $^1\text{O}_2$ in organic media.

EXPERIMENTAL SECTION

Standard Procedure for Synthesis of 1,1-Dihydroperoxides.

1,1-Dihydroperoxides were prepared by a reported procedure.²⁴

1,1-Dihydroperoxy-4-tert-butylcyclohexane (1a): 84%, white solid; mp 81–83 °C; $R_f = 0.33$ (30% EA/Hex); other physical data were identical to literature reports.²⁴

1,1-Dihydroperoxycycloheptane (2a): 83%, white solid; mp 59–61 °C; $R_f = 0.33$ (30% EA/Hex); other physical data were identical to literature reports.²⁴

1,1-Dihydroperoxycyclooctane (3a): 58%, colorless oil; $R_f = 0.33$ (30% EA/Hex); other physical data were identical to literature reports.²⁴

4-Phenyl-2,2-dihydroperoxybutane (4a): 72%, white solid; mp 61–63 °C; $R_f = 0.36$ (40% EA/Hex); other physical data were identical to literature reports.²⁴

1,1-Dihydroperoxyadamantane (5a): 88%, white solid; mp 148–150 °C; $R_f = 0.30$ (30% EA/Hex); other physical data were identical to literature reports.²⁴

5,5-Dihydroperoxynonane (6a): 75%, colorless oil; $R_f = 0.25$ (20% EA/Hex); other physical data were identical to literature reports.²⁴

1,1-Dihydroperoxy-3-tert-butylcyclopentane (7a): 84%, colorless oil; $R_f = 0.30$ (30% EA/Hex); IR 3420, 2956, 2870, 1365, 1104, 963 cm^{-1} ; $^1\text{H NMR}$ δ 9.83 (s, 2H), 2.05 (m, 2H), 1.9 (m, 2H), 1.7 (m, 2H), 1.47 (m, 1H), 0.85 (s, 9H); $^{13}\text{C NMR}$ δ 121.7, 49.2, 34.5, 32.6,

31.5, 27.4, 25.6; HRMS (ESI, MeOH/H₂O, NaOAc) calcd for C₉H₁₈NaO₄ (M + Na)⁺ 213.1103, found 213.1110.

1,1-Dihydroperoxycyclododecane (8a): 93%, colorless oil; *R_f* = 0.33 (30% EA/Hex); other physical data were identical to literature reports.²⁴

Standard Procedure for Preparation of 1,1-Dihydroperoxide Monoacetates (Illustrated for 1b). To a solution of 4-*tert*-butylcyclohexyl-1,1-dihydroperoxide **1a** (1.48 g, 7.2 mmol) in CH₂Cl₂ (15 mL) were added DMAP (0.09 g, 0.75 mmol) and pyridine (0.57 g, 7.2 mmol). The reaction mixture was cooled to 0 °C, and a solution of Ac₂O (0.74 g, 7.2 mmol) in CH₂Cl₂ (10 mL) was added dropwise over 10 min. Upon completion of addition, the reaction was stirred for 30 min at 0 °C and then diluted with CH₂Cl₂ (100 mL). The solution was washed with saturated NaHCO₃ (20 mL), water (20 mL), and brine (20 mL) and then dried over anhydrous Na₂SO₄. The residue obtained upon removal of the solvent in vacuo was purified by silica flash chromatography (5% EA/Hex) to give a white solid (1.47 g, 84% yield). The acid anhydride could be replaced by acid chloride (peresters) or ethoxycarbonyl chloride (percarbonates) without any other change.

1-Acetyldioxy-1-hydroperoxy-4-*tert*-butylcyclohexane (1b): 84%, white solid; mp 35–37 °C; *R_f* = 0.33 (10% EA/Hex); other physical data were identical to literature reports.²³

1-Acetyldioxy-1-hydroperoxycycloheptane (2b): 76%, colorless oil; *R_f* = 0.33 (10% EA/Hex); IR 3345, 2930, 2859, 1756, 1425, 1171, 1006, 899 cm⁻¹; ¹H NMR δ 10.13 (s, 1H), 2.09 (2, 3H), 1.92 (m, 4H), 1.54 (br, 8H); ¹³C NMR δ 171.7, 117.4, 32.5, 29.6, 22.6, 17.5; HRMS (ESI, MeOH/H₂O, NaOAc) calcd for C₉H₁₆NaO₅ (M + Na)⁺ 227.0895, found 227.0898.

1-Acetyldioxy-1-hydroperoxycyclooctane (3b): 73%, colorless oil; *R_f* = 0.33 (10% EA/Hex); IR 3340, 2924, 1756, 1409, 1200, 1078, 898 cm⁻¹; ¹H NMR δ 10.13 (s, 1H), 2.15 (s, 3H), 2.00 (m, 2H), 1.89 (m, 2H), 1.63 (br, 4H), 1.57 (br, 6H); ¹³C NMR δ 171.7, 116.8, 27.8, 27.4, 24.9, 21.8, 17.6; HRMS (ESI, MeOH/H₂O, NaOAc), calcd for C₁₀H₁₈NaO₅ (M + Na)⁺ 241.1052, found 241.1046.

4-Phenyl-1-acetyldioxy-1-hydroperoxybutane (4b): 86%, colorless oil; *R_f* = 0.33 (10% EA/Hex); IR 3340, 2988, 2900, 1758, 1378, 1066, 899, 748, 698 cm⁻¹; ¹H NMR δ 10.39 (s, 1H), 7.35 (m, 2H), 7.28 (m, 3H), 2.86 (m, 2H), 2.24 (dd, *J* = 5.46, 12.9 Hz, 1H), 2.20 (s, 3H), 2.09 (dd, *J* = 5.46, 12.2 Hz, 1H), 1.61 (s, 3H); ¹³C NMR δ 171.7, 141.0, 128.6, 128.4, 126.3, 113.7, 34.9, 30.2, 18.1, 17.6; HRMS (ESI, MeOH/H₂O, NaOAc) calcd for C₁₂H₁₆NaO₅ (M + Na)⁺ 263.0895, found 263.0899.

5-Acetyldioxy-5-hydroperoxyononane (6b): 76%, colorless oil; *R_f* = 0.33 (10% EA/Hex); IR 3350, 2960, 2873, 1760, 1198, 1056, 899 cm⁻¹; ¹H NMR δ 10.13 (s, 1H), 2.12 (s, 3H), 1.73 (m, 2H), 1.56 (m, 2H), 1.34 (m, 8H), 0.90 (t, *J* = 7.15 Hz, 3H); ¹³C NMR δ 171.6, 116.0, 28.9, 25.6, 22.7, 17.4, 13.8; HRMS (ESI, MeOH/H₂O, NaOAc) calcd for C₁₁H₂₂NaO₅ (M + Na)⁺ 257.1365, found 257.1361.

1-Acetyldioxy-1-hydroperoxy-3-*tert*-butylcyclopentane (7b): 84%, colorless oil; *R_f* = 0.33 (10% EA/Hex); IR 2959, 2869, 1758, 1365, 1184, 1070, 962; ¹H NMR δ 10.516/10.501 (two s, totaling 1H), 2.17 (s, 3H), 2.0 (m, 4H), 1.75 (m, 2H), 1.54 (m, 1H), 0.88 (s, 9H); ¹³C NMR δ 171.6, 122.9, 122.8, 49.3, 49.2, 34.6, 34.5, 32.7, 32.6, 31.6, 27.38, 27.36, 25.6, 17.6; HRMS (ESI, MeOH/H₂O, NaOAc) calcd for C₁₁H₂₀NaO₅ (M + Na)⁺ 255.1208, found 255.1199.

1-Acetyldioxy-1-hydroperoxycyclododecane (8b): 81%, colorless oil; *R_f* = 0.33 (10% EA/Hex); IR 3307, 2946, 2851, 1748, 1426, 1190, 997, 850 cm⁻¹; ¹H NMR δ 10.22 (s, 1H), 2.17 (s, 3H), 1.76 (m, 2H), 1.59 (m, 6H), 1.39 (br, 14H); ¹³C NMR δ 171.7, 116.8, 26.1, 25.9, 25.8, 22.1, 21.8, 19.3, 17.7; HRMS (ESI, MeOH/H₂O, NaOAc) calcd for C₁₄H₂₆NaO₅ (M + Na)⁺ 297.1678, found 297.1679.

1-Benzoyldioxy-1-hydroperoxy-4-*tert*-butylcyclohexane (1c): 37%, white solid; mp 76–78 °C; *R_f* = 0.43 (10% EA/Hex); other physical data were identical to literature reports.²³

4-*tert*-Butyl-1-hydroperoxycyclohexyl ethyl carbonperoxoate (1d): 76%, colorless oil; *R_f* = 0.22 (10% EA/Hex); other physical data were identical to literature reports.²³

Standard Procedure for Preparation of Monosilylated Peresters (Illustrated for 9a). To a solution of monoacetate **1b**

(2.46 g, 10 mmol) in CH₂Cl₂ (150 mL) were added DMAP (0.24 g, 2.0 mmol) and Et₃N (2.7 mL, 20 mmol). The reaction mixture was cooled to 0 °C, and a solution of TESCl (1.5 g, 10 mmol) in CH₂Cl₂ (50 mL) was added dropwise over 10 min. The reaction was stirred for 30 min at 0 °C, and then the solvent was removed in vacuo. The residue obtained was purified by silica flash chromatography (5% EA/Hex) to give a colorless, oily product (2.09 g, 58% yield).

1-Acetyldioxy-1-triethylsilyldioxy-4-*tert*-butylcyclohexane (9a): 58%, colorless oil; *R_f* = 0.65 (20% EA/Hex); IR 2954, 1777, 1366, 1180, 865 cm⁻¹; ¹H NMR δ 2.33 (d, *J* = 14.48 Hz, 2H), 2.15 (s, 3H), 1.70 (d, *J* = 13.2 Hz, 2H), 1.46 (dt, *J* = 3.78, 13.8 Hz, 2H), 1.30 (m, 2H), 1.05 (m, 1H), 0.98 (t, *J* = 7.69 Hz, 9H), 0.87 (s, 9H), 0.69 (dd, *J* = 7.55, 16.27 Hz, 6H); ¹³C NMR (233K) δ 167.9, 110.6, 47.2, 32.5, 30.4, 27.7, 23.2, 18.3, 7.0, 3.4; HRMS (ESI, MeOH/H₂O, NaOAc) calcd for C₁₈H₃₆NaO₅Si (M + Na)⁺ 383.2230, found 383.2224.

1-Acetyldioxy-1-*tert*-butyldimethylsilyldioxy-4-*tert*-butylcyclohexane (9b). TESCl was replaced by TBSCl without any other change: 65%, colorless oil; *R_f* = 0.65 (20% EA/Hex); IR 2954, 2859, 1777, 1365, 1178, 873, 830, 784 cm⁻¹; ¹H NMR δ 2.33 (m, 2H), 2.14 (s, 3H), 1.68 (m, 2H), 1.46 (dt, *J* = 3.85, 13.63 Hz, 2H), 1.29 (m, 2H), 1.05 (m, 1H), 0.93 (s, 9H), 0.87 (s, 9H), 0.14 (s, 6H); ¹³C NMR (233K) δ 167.9, 110.7, 47.2, 32.5, 30.4, 27.7, 26.3, 23.2, 18.6, 18.3; HRMS (ESI, MeOH/H₂O, NaOAc) calcd for C₁₈H₃₆NaO₅Si (M + Na)⁺ 383.2230, found 383.2235.

1-Acetyldioxy-1-triethylsilyldioxycycloheptane (10): 81%, colorless oil; *R_f* = 0.65 (20% EA/Hex); IR 2969, 1776, 1409, 1170, 1056, 796 cm⁻¹; ¹H NMR δ 2.08 (s, 3H), 1.95 (m, 4H), 1.55 (br, 8H), 0.97 (t, *J* = 7.86 Hz, 9H), 0.68 (q, 6H); ¹³C NMR δ 115.9, 33.0, 30.2, 22.8, 17.8, 6.6, 3.7; HRMS (ESI, MeOH/H₂O, NaOAc) calcd for C₁₅H₃₀NaO₅Si (M + Na)⁺ 341.1760, found 341.1759.

1-Acetyldioxy-1-triethylsilyldioxycyclooctane (11): 70%, colorless oil; *R_f* = 0.65 (20% EA/Hex); IR 2956, 1776, 1363, 1184, 1066, 833, 729 cm⁻¹; ¹H NMR δ 2.10 (s, 3H), 1.97 (m, 4H), 1.56 (br, 10H), 0.97 (t, *J* = 7.63 Hz, 9H), 0.68 (q, 6H); ¹³C NMR (233K) δ 168.1, 115.0, 27.8, 27.2, 24.7, 22.0, 18.2, 7.0, 3.7; HRMS (ESI, MeOH/H₂O, NaOAc) calcd for C₁₆H₃₂NaO₅Si (M + Na)⁺ 355.1917, found 355.1906.

4-Phenyl-1-acetyldioxy-1-triethylsilyldioxybutane (12): 79%, colorless oil; *R_f* = 0.65 (20% EA/Hex); IR 2957, 1780, 1182, 1103, 825, 698 cm⁻¹; ¹H NMR δ 7.31 (m, 2H), 7.23 (m, 2H), 2.78 (t, *J* = 8.95 Hz, 2H), 2.15 (m, 5H), 1.57 (s, 3H), 1.04 (t, *J* = 7.95 Hz, 9H), 0.75 (q, 6H); ¹³C NMR δ 141.3, 128.5, 128.3, 126.1, 111.9, 35.5, 30.4, 18.5, 17.8, 6.7, 3.7; HRMS (ESI, MeOH/H₂O, NaOAc) calcd for C₁₈H₃₀NaO₅Si (M + Na)⁺ 377.1760, found 377.1756.

1-Acetyldioxy-1-triethylsilyldioxyononane (13): 73%, colorless oil; *R_f* = 0.65 (20% EA/Hex); IR 2959, 1781, 1409, 1184, 1066, 802, 729 cm⁻¹; ¹H NMR δ 2.04 (s, 2H), 1.69 (m, 2H), 1.30 (br, 8H), 0.93 (t, *J* = 7.85 Hz, 9H), 0.85 (t, *J* = 6.35 Hz, 6H), 0.63 (q, 6H); ¹³C NMR δ 114.1, 29.6, 25.5, 22.7, 17.7, 13.7, 6.5, 3.6; HRMS (ESI, MeOH/H₂O, NaOAc) calcd for C₁₈H₃₀NaO₅Si (M + Na)⁺ 377.1760, found 377.1768.

1-Acetyldioxy-1-triethylsilyldioxycyclododecane (14): 80%, colorless oil; *R_f* = 0.65 (20% EA/Hex); IR 2929, 1779, 1470, 1186, 1003, 851, 728 cm⁻¹; ¹H NMR δ 2.08 (s, 3H), 1.73 (m, 4H), 1.37 (br, 18H), 0.96 (t, *J* = 7.96 Hz, 9H), 0.66 (q, 6H); ¹³C NMR δ 114.9, 26.7, 26.1, 26.0, 22.3, 21.9, 19.4, 6.7, 3.7; HRMS (ESI, MeOH/H₂O, NaOAc) calcd for C₂₀H₄₀NaO₅Si (M + Na)⁺ 411.2543, found 411.2536.

1,1-Triethylsilyldioxy-4-*tert*-butylcyclohexane (15). To a solution of 4-*tert*-butylcyclohexyl-1,1-dihydroperoxide **1a** (0.50 g, 2.5 mmol) in DMF (30 mL) was added Et₃N (0.76 mL, 5.4 mmol). The reaction mixture was cooled to -40 °C, and TESCl (0.91 mL, 5.4 mmol) was added. The reaction was stirred for 1 h at -40 °C and then quenched with brine (100 mL). The solution was extracted with hexane (50 mL) three times, and the combined organic layer was dried over anhydrous Na₂SO₄. The residue obtained upon removal of the solvent in vacuo was purified by silica flash chromatography (5% EA/Hex) to give a colorless oil (0.57 g, 53%), *R_f* = 0.80 (20% EA/Hex); other physical data were identical to literature reports.⁴²

1,1-Diacetyldioxy-4-*tert*-butylcyclohexane (16). To a solution of 4-*tert*-butylcyclohexyl-1,1-dihydroperoxide **1a** (1.48 g, 7.2 mmol) in

CH_2Cl_2 (15 mL) were added DMAP (0.09 g, 0.75 mmol), and pyridine (0.57 g, 7.2 mmol). The reaction mixture was cooled to 0 °C, and a solution of Ac_2O (1.48 g, 14.4 mmol) in CH_2Cl_2 (10 mL) was added dropwise over 10 min. Upon completion of addition, the reaction was stirred for 30 min at 0 °C and then diluted with CH_2Cl_2 (100 mL). The solution was washed with saturated NaHCO_3 (20 mL), water (20 mL), and brine (20 mL) and then dried over anhydrous Na_2SO_4 . The residue obtained upon removal of the solvent in vacuo was purified by silica flash chromatography (10% EA/Hex) to give a white solid (1.55 g, 75% yield): mp 54–56 °C; R_f = 0.30 (20% EA/Hex); IR 2960, 2869, 1785, 1361, 1187, 1057, 896 cm^{-1} ; ^1H NMR δ 2.34 (d, J = 12.81 Hz, 2H), 2.08 (s, 3H), 2.07 (s, 3H), 1.75 (d, J = 14.12 Hz, 2H), 1.62 (m, 2H), 1.31 (m, 2H), 1.09 (m, 1H), 0.86 (s, 9H); ^{13}C NMR δ 167.5, 167.4, 111.5, 47.1, 32.2, 30.1, 27.5, 23.2, 17.5, 17.4; HRMS (ESI, MeOH/ H_2O , NaOAc) calcd for $\text{C}_{14}\text{H}_{24}\text{NaO}_6$ ($\text{M} + \text{Na}$)⁺ 311.1471, found 311.1467.

NMR Method for Quantification of Oxygen Transfer (Illustrated for Dioxygenation of Terpinene). To a solution of **1b** (50 mg, 0.2 mmol) and α -terpinene (**T**, 90%, 15 mg, 0.1 mmol) in CH_3CN (2 mL) was injected TBAF (1 M in THF, 0.24 mL, 0.24 mmol) within 5 s and the reaction mixture stirred at room temperature for 5 min. Solvent was removed by vacuum. Internal standard 1,2-dichloroethane was added, and **T-O₂** was measured by NMR. The alkene peak at 6.3 ppm (dd, J = 8.56, 25.93 Hz) of **T-O₂** will be used for calculation via following equations:

$$\text{actual mole}_{\text{T-O}_2} = \text{mole}_{\text{standard}} \cdot 2 \cdot \text{area}_{\text{T-O}_2} / \text{area}_{\text{standard}}$$

Therefore, the calculated % yield = $100 \cdot \text{actual mole}_{\text{T-O}_2} / \text{theoretical mole}_{\text{T-O}_2}$.

Alternatively, quantification of **T-O₂** can be conducted by GC/MS using a reported procedure⁵

GC/MS Quantification of Relative Reactivity of Dihydroperoxide Monoesters (Illustrated for **1b and **4b**).** Prepare a standard solution of 4-*tert*-butylcyclohexanone (1 mmol) and benzylacetone (1 mmol) in CH_3CN (2 mL). The standard ratio α = $\text{area}_{4\text{-tert-butylcyclohexanone standard}} / \text{area}_{\text{benzylacetone standard}}$. The mole ratio of the ketone products from the competitive reaction is $\text{area}_{4\text{-tert-butylcyclohexanone actual}} / (\alpha \cdot \text{area}_{\text{benzylacetone actual}})$.

Sample Procedure for Oxygen Transfer (Illustrated for Decomposition of **1b and Dioxygenation of Terpinene).** To a solution of **1b** (50 mg, 0.20 mmol) and α -terpinene (**T**, 90%, 15 mg, 0.10 mmol) in CH_3CN (2 mL) was added via syringe a solution of TBAF (nominally 1 M in THF, 0.24 mL, 0.24 mmol) over 5 s. The reaction mixture was stirred at room temperature for 5 min and then the solvent was removed under vacuum. 1,2-Dichloroethane was added as an internal standard and **T-O₂** determined by NMR, GC/MS, or isolation, as described in the Supporting Information.

Standard Procedure for Fluoride-Mediated Decomposition of Silylated Monoesters. To a solution of **9a** (77 mg, 0.2 mmol) and 1,3-diphenylisobenzofuran (DPBF, **D**, 27 mg, 0.10 mmol) in CH_3CN (2 mL) was added via syringe a solution of TBAF (nominally 1 M in THF, 0.24 mL, 0.24 mmol) and the reaction mixture stirred at room temperature for 5 min. Then solvent was removed by vacuum, and the residue was purified by column chromatography on silica gel to give the pure product **D-O₂** (19 mg, 66%).

Standard Procedure for Tandem Activation and Decomposition of 1,1-Dihydroperoxides (Illustrated for Trichloroacetonitrile). To a solution of **1a** (41 mg, 0.2 mmol), CCl_3CN (29 mg, 0.2 mmol), and 1,3-diphenylisobenzofuran (DPBF, **D**, 27 mg, 0.1 mmol) in CH_3CN (2 mL) was added KOTu (90 mg, 0.8 mmol). The reaction was monitored by TLC and stirred at room temperature for 5 min. Then solvent was removed by vacuum, and the residue was purified by column chromatography on silica gel to give the pure product **D-O₂** (21 mg, 72% yield based upon **D** or 36% based upon consumed 1,1-dihydroperoxide).

Calculation Methods. The B3LYP/6-31+G(d,p) model chemistry was used in all calculations. Differences in electronic energies were corrected by inclusion of zero-point vibrational energies scaled by 0.9806. Because B3LYP is based on a single Slater determinant, it cannot rigorously describe either singlet molecular oxygen or transition states in which states O_2 is a distinct moiety. The standard

approximate treatment is to relax the restriction that α and β orbitals be identical. While this allows B3LYP to provide a qualitatively correct description of the electronic structure, this treatment also introduces triplet character into the wave function. We corrected for this spin contamination using the approach of Houk and co-workers.⁴³ This approach predicts a singlet–triplet gap for molecular oxygen of 20.8 kcal/mol, in fair agreement with the experimental value of 22.5 kcal/mol.^{1a} Individual conformers within the monoperoacetate and monopercarbonate systems, along with optimized coordinates for each minimized structure or transition state, are described in the Supporting Information.

■ ASSOCIATED CONTENT

📄 Supporting Information

Details regarding experimental procedures, spectral listings for new molecules, ^1H and ^{13}C NMR data for new compounds, thermal analysis for **1a** and **1c**, conformational analysis of model monoperoxyacetate and monopercarbonate structures, and optimized coordinates of calculated structures described in the paper. This material is available free of charge via the Internet at <http://pubs.acs.org>.

■ AUTHOR INFORMATION

Corresponding Author

*E-mail: pdussault1@unl.edu.

Present Address

[§]Department of Chemistry, Indian Institute of Science and Education Research, Bhopal, India.

■ ACKNOWLEDGMENTS

Research was conducted with funding from NSF (CHE-0749916, –1057982) and the Camille and Henry Dreyfus Foundation in facilities remodeled with NIH support (RR016544). Calculations were performed at Macalester College, the National Center for Supercomputing Applications facility at the University of Illinois (CHE090078), and the Midwest Undergraduate Computational Chemistry Consortium facility at Hope College (NSF-CHE-0520704). We thank Dr. Joe Dumais and Prof. Charles Kingsbury for useful discussions.

■ REFERENCES

- (1) (a) Foote, C. S.; Clennan, E. L. In *Active Oxygen in Chemistry*; Foote, C. S., Valentine, J. S., Greenberg, A., Liebman, J. F., Eds.; Blackie Academic and Professional: London, 1995; p 105. (b) Clennan, E.; Pace, A. *Tetrahedron* **2005**, *61*, 6665. (c) Endo, M. *Russ. J. Phys. Chem. A* **2007**, *81*, 1497.
- (2) Gollnick, K.; Kuhn, H. J. In *Singlet Oxygen*; Wasserman, H. H., Murray, R. W., Eds.; Academic Press: New York, 1979; pp 287–427.
- (3) Clennan, E. L.; L'Esperance, R. P. *Tetrahedron Lett.* **1983**, *24*, 4291.
- (4) Sheu, C.; Kang, P.; Khan, S.; Foote, C. S. *J. Am. Chem. Soc.* **2002**, *124*, 3905.
- (5) Schmidt, R. *Photochem. Photobiol.* **2006**, *82*, 1161.
- (6) Wootton, R. C. R.; Fortt, R.; de Mello, A. J. *Org. Process Res. Dev.* **2002**, *6*, 187.
- (7) Foote, C. S.; Wexler, S.; Ando, W.; Higgins, R. J. *Am. Chem. Soc.* **1968**, *90*, 975. Greer, A. *Acc. Chem. Res.* **2006**, *39*, 797.
- (8) Jary, W. G.; Ganglberger, T.; Pöchlauer, P.; Falk, H. *Monatsh. Chem.* **2005**, *136*, 537. Ganglberger, T.; Jary, W. G.; Pöchlauer, P.; Aubry, J.-M.; Nardello, V.; Falk, H. *Monatsh. Chem.* **2004**, *135*, 501.
- (9) Adam, W.; Kazakov, D. V.; Kazakov, V. P. *Chem. Rev.* **2005**, *105*, 3371. Wahlen, J.; De Vos, D. E.; Jacobs, P. A.; Alsters, P. L. *Adv. Synth. Catal.* **2004**, *346*, 152.

- (10) Catir, M.; Kilic, H.; Nardello-Rataj, V.; Aubry, J.-M.; Kazaz, C. *J. Org. Chem.* **2009**, *74*, 4560.
- (11) Sels, B. F.; De Vos, D. E.; Jacobs, P. A. *J. Am. Chem. Soc.* **2007**, *129*, 6916.
- (12) Nardello, V.; Barbillat, J.; Marko, J.; Witte, P. T.; Alsters, P. L.; Aubry, J.-M. *Chem.—Eur. J.* **2003**, *9*, 435.
- (13) Renirie, R.; Pierlot, C.; Aubry, J.-M.; Hartog, A. F.; Schoemaker, H. E.; Alsters, P. L.; Wever, R. *Adv. Synth. Catal.* **2003**, *345*, 849.
- (14) Corey, E. J.; Mehrotra, M. M.; Khan, A. U. *J. Am. Chem. Soc.* **1986**, *108*, 2472. Posner, G. H.; Weitzberg, M.; Nelson, W. M.; Murr, B. L.; Seliger, H. H. *J. Am. Chem. Soc.* **1987**, *109*, 278. Cerkovnik, J.; Tuttle, T.; Kraka, E.; Lendero, N.; Plesnicar, B.; Cremer, D. *J. Am. Chem. Soc.* **2006**, *128*, 4090.
- (15) Deslongchamps, P.; Atlani, P.; Fréhel, D.; Malaval, A.; Moreau, C. *Can. J. Chem.* **1974**, *52*, 3651. Abdrakhmanova, A. R.; Khalitova, L. R.; Spirikhin, L. V.; Dokichev, V. A.; Grabovskiy, S. A.; Kabal'nova, N. N. *Russ. Chem. Bull. Int. Ed.* **2007**, *56*, 271.
- (16) Pierlot, C.; Nardello, V.; Schrive, J.; Mabile, C.; Barbillat, J.; Sombret, B.; Aubry, J.-M. *J. Org. Chem.* **2002**, *67*, 2418.
- (17) Carreño, M. C.; González-Lopez, M.; Urbano, A. *Angew. Chem., Int. Ed.* **2006**, *45*, 2737.
- (18) The half-life of $^1\text{O}_2$ ranges from 1–2 μs in H_2O to 60 μs in CH_3CN to nearly milliseconds in perhalogenated solvents. See ref 1a and Wilkinson, F.; Helman, W. P.; Ross, A. B. *J. Phys. Chem. Ref. Data* **1995**, *24*, 663.
- (19) See, for example: Aubry, J.-M.; Adam, W.; Alsters, P. L.; Borde, C.; Queste, S.; Marko, J.; Nardello, V. *Tetrahedron* **2006**, *62*, 10753. Caron, L.; Nardello, V.; Alsters, P. L.; Aubry, J.-M. *J. Mol. Catal. A: Chem.* **2006**, *251*, 194.
- (20) Aubry, J.-M.; Pierlot, C.; Rigaudy, J.; Schmidt, R. *Acc. Chem. Res.* **2003**, *36*, 668.
- (21) Thompson, Q. E. *J. Am. Chem. Soc.* **1961**, *83*, 845. Mendenhall, G. D. In *Advances in Oxygenated Processes*; Baumstark, A. L., Ed.; JAI: Greenwich, 1990; Vol. 2, p 203.
- (22) Schwartz, C.; Raible, J.; Mott, K.; Dussault, P. H. *Org. Lett.* **2006**, *8*, 3199; *Tetrahedron* **2006**, *62*, 10747.
- (23) Ghorai, P.; Dussault, P. H. *Org. Lett.* **2009**, *11*, 4572.
- (24) Ghorai, P.; Dussault, P. H. *Org. Lett.* **2008**, *10*, 4577.
- (25) Cudden, R. C. P.; Hewlett, C. J. *Chem. Soc. C* **1968**, 2983. Dihydroperoxide monoesters have been investigated as radical initiators: Van de Bovenkamp-Bouwman, A. G.; Van Gendt, J. W. J.; Meijer, J.; Hogt, A. H.; Van Swieten, A. P. PCT Int. Appl. WO 9932442 A1 19990701, 1999.
- (26) Dussault, P. H. In *Active Oxygen in Chemistry*; Foote, C. S., Valentine, J. S., Greenberg, A., Liebman, J. F., Eds.; Blackie A&P: London, 1995; pp 141–203.
- (27) The rate constants for reaction of $^1\text{O}_2$ with terpinene and 1,3-diphenylisobenzofuran (DPBF, **D**) are on the order of 10^8 and 10^9 L/mol-s, respectively; see ref 18. *Caution*: DPBF is both an efficient $^1\text{O}_2$ trap and a visible photosensitizer. In control reactions, we found that stirring a solution of **1b** with DPBF in an unlit fume hood gave little oxidized product (**D-O₂**) over the typical period (≤ 0.5 h) of these reactions. In contrast, care had to be taken to prevent extensive formation of **D-O₂** during chromatographic purification of reaction mixtures under normal laboratory lighting. See: Nowakowska, M. *J. Chem. Soc., Faraday Trans. 1* **1984**, *80*, 2119; Howard, J. A.; Mendenhall, G. D. *Can. J. Chem.* **1975**, *53*, 2199. No precautions were required with terpinene (**T**).
- (28) Miller, J.; Abernathy, S.; Sharp, R. *J. Phys. Chem. A* **2000**, *104*, 4839.
- (29) Bis perester derivatives of 1,1-dihydroperoxides have been prepared: Criegee, R.; Schnorrenberg, W.; Becke, J. *Annalen* **1949**, *565*, 7. Warnant, J.; Joly, R.; Mathieu, J.; Velluz, L. *Bull. Soc. Chim. Fr.* **1957**, 331. Milas, N. A.; Golubovic, A. *J. Am. Chem. Soc.* **1959**, *81*, 6461. They have also been investigated as polymerization initiators: Van de Bovenkamp-Bouwman, A. G.; Van Gendt, J. W. J.; Meijer, J.; Hogt, A. H.; Van Swieten, A. P. (Akzo Nobel N.V., Neth.) PCT Int. Appl. 1999, 42 pp. CODEN: PIXXD2 WO 9932442 A1 19990701.
- (30) Davies, A. G.; Sutcliffe, R. J. *J. Chem. Soc., Perkins Trans. 2* **1981**, 1512.
- (31) (a) Grob, C. A.; Bolleter, M.; Kunz, W. *Angew. Chem., Int. Ed. Engl.* **1980**, *19*, 708. (b) Grob, C. A. *Angew. Chem., Int. Ed. Engl.* **1969**, *8*, 535.
- (32) Baader, W. J. In *Science of Synthesis*; Berkessel, A., Ed.; Georg Thieme Verlag: Stuttgart, 2009; Vol. 38 (Four-Membered Ring Cyclic Peroxides), pp 323–344.
- (33) Adam, W.; Curci, R.; Edwards, J. O. *Acc. Chem. Res.* **1989**, *22*, 205. Murray, R. W. *Chem. Rev.* **1989**, *89*, 1187.
- (34) All identified conformers are described within the Supporting Information.
- (35) Tâme Parreira, R. L.; Galembeck, S. E.; Hobza, P. *Chem. Phys. Chem.* **2007**, *8*, 87.
- (36) The successful alkylation of 1,1-dihydroperoxides using CsOH also demonstrates the stability of 1,1-dihydroperoxides and 1-alkyldioxy-1-hydroperoxyalkanes toward strongly basic conditions, although it is interesting to note that ketones are obtained as minor byproducts in these reactions: Hamada, Y.; Tokuhara, H.; Masuyama, A.; Nojima, M.; Kim, H.-S.; Ono, K.; Ogura, N.; Wataya, Y. *J. Med. Chem.* **2002**, *45*, 1374.
- (37) Payne, G. B. *Tetrahedron* **1962**, *18*, 763. Payne, G. B.; Deming, P. H.; Williams, P. H. *J. Org. Chem.* **1961**, *26*, 659.
- (38) Long, C. A.; Kearns, D. R. *J. Am. Chem. Soc.* **1975**, *97*, 2018.
- (39) Frimer, A. A. *Chem. Rev.* **1979**, *79*, 359. Gorman, A. A.; Gould, I. R.; Hamblet, I. J. *J. Am. Chem. Soc.* **1982**, *104*, 7098.
- (40) Matheson, I. B. C.; Lee, J.; Yamashita, B. S.; Wolbarsht, M. L. *Chem. Phys. Lett.* **1974**, *27*, 355.
- (41) (a) Criegee: Goodman, R. M.; Kishi, Y. *J. Am. Chem. Soc.* **1998**, *120*, 9392. Criegee, R. *Lieb. Ann.* **1948**, *560*, 127. Kropf, H. In *Methoden der Organischen Chemie*, 4th ed.; Kropf, H., Ed.; Thieme: Stuttgart, 1988; Vol. E13; pp 1095–1099; (b) Hock: Hock, H.; Kropf, H. *Angew. Chem.* **1957**, *69*, 313. Dussault, P. H.; Lee, H. J.; Liu, X. *Perkin* **2000**, *1*, 3006. (c) Anomalous ozonolysis: Jung, M. E.; Davidov, P. *Org. Lett.* **2001**, *3*, 627. (d) Fragmentation of 2-hydroperoxy acids: Richardson, W. H.; Smith, R. S. *J. Am. Chem. Soc.* **1967**, *89*, 2230.
- (42) Ramirez, A.; Woerpel, K. A. *Org. Lett.* **2005**, *7*, 4617.
- (43) Goldstein, E.; Beno, B.; Houk, K. N. *J. Am. Chem. Soc.* **1996**, *118*, 6036.